The Astrophysical Journal, 698:L188–L191, 2009 June 20 doi:10.1088/0004-637X/698/2/L188
© 2009. The American Astronomical Society. All rights reserved. Printed in the U.S.A.

RESOLVED DUST EMISSION IN A QUASAR AT $z = 3.65$

D. L. Clements[1], G. Petitpas[2], D. Farrah[3], E. Hatziminaoglou[4,5], T. Babbedge[1], M. Rowan-Robinson[1], I. Pérez-Fournon[5], Antonio Hernán-Caballero[5], Nieves Castro-Rodríguez[5], C. Lonsdale[6], J. Surace[7], A. Franceschini[8], B. J. Wilkes[9], and H. Smith[10]

[1] Physics Department, Imperial College, Prince Consort Road, London SW7 2AZ, UK
[2] Submillimetre Array, Hilo, HI, USA
[3] Astronomy Centre, University of Sussex, Brighton, BN1 9QH, UK
[4] European Southern Observatory, Garching, Munich, Germany
[5] IAC, Tenerife, Spain
[6] IPAC, Caltech, Pasadena, CA, USA
[7] Spitzer Science Centre, Caltech, Pasadena, CA, USA
[8] Universita di Padova, Padova, Italy
[9] Harvard-Smithsonian Centre for Astrophysics, Cambridge, MA, USA
[10] UCSD, San Diego, CA, USA

Received 2009 March 10; accepted 2009 May 11; published 2009 June 5

ABSTRACT

We present submillimeter observations of the $z = 3.653$ quasar SDSS 160705+533558 together with data in the optical and infrared. The object is unusually bright in the far-IR and submillimeter with an IR luminosity of $\sim 10^{14}\ L_{\odot}$. We ascribe this luminosity to a combination of active galactic nucleus (AGN) and starburst emission, with the starburst forming stars at a rate of a few thousand solar masses per year. Submillimeter Array imaging observations with a resolution $\sim 1''$ show that the submillimeter (850 μm) emission is extended on scales of 10–35 kpc and is offset from the optical position by ~ 10 kpc. This morphology is dissimilar to that found in submillimeter galaxies, which are generally unresolved or marginally resolved on arcsecond scales, or submillimeter-luminous AGNs where the AGN lies at the peak of the submillimeter or molecular emission. The simplest explanation is that the object is in the early stages of a merger between a gas-rich galaxy, which hosts the starburst, and a gas-poor AGN-host galaxy, which is responsible for the quasar emission. It is also possible that jet-induced star formation might contribute to the unusual morphology.

Key words: galaxies: high-redshift – galaxies: interactions – galaxies: starburst – quasars: individual (SDSS 160705+533558) – submillimeter

1. INTRODUCTION

Understanding the rest-frame far-IR properties of high-redshift galaxies and quasars has become a major field, inspired by the detection of the Cosmic Infrared Background (CIB; Puget et al. 1996; Fixsen et al. 1998), and by the unexpectedly large number of distant submillimeter sources in Submillimeter Common-User Bolometric Array (SCUBA) surveys (e.g., Hughes et al. 1998; Smail et al. 1997; Eales et al. 2000; Coppin et al. 2006). Much of the far-IR emission in these objects appears to be produced by dust-obscured starbursts (Alexander et al. 2005; Clements et al. 2008; Dye et al. 2008) similar to local ultraluminous infrared galaxies (ULIRGs). While starbursts dominate the bolometric output of these systems, they may still contain active galactic nuclei (AGNs). Spectral energy distribution (SED) analysis of local ULIRGs (e.g., Farrah et al. 2003) reveals that at least half contain an AGN, a figure confirmed by mid-IR spectral studies (Armus et al. 2007; Farrah et al. 2007; Desai et al. 2007). Meanwhile, correlations between galaxy bulge and supermassive black hole masses suggest that star formation and AGN fueling are intimately linked (Haring & Rix 2004). Studies of sources containing both starbursts and AGN probe this link. A number of far-IR luminous high-z AGNs are already known (e.g., Priddey et al. 2003), some of which have associated submillimeter sources. Separations between submillimeter and AGN components in these sources cover the full range of scales on which submillimeter emission can be resolved, ranging from 400 kpc (Stevens et al. 2004) for sources observed by SCUBA (resolution $15''$) to $4''$ for the famous resolved submillimeter-luminous AGN BR1202-0725 at $z = 4.69$ (Omont et al. 1996).

As part of efforts to understand the links between star formation and AGN activity at high redshift, we have been searching for $z > 3$ objects that show evidence for both an AGN, and for a far-IR excess, and observing them at submillimeter wavelengths. One such object is SDSS 160705+533558, a quasar found in the Sloan Digital Sky Survey (SDSS), with a spectroscopic redshift of $z = 3.653$. It was observed during the *Spitzer* SWIRE survey (Lonsdale et al. 2004) and detected at 70 μm and all shorter *Spitzer* bands (Hatziminaoglou et al. 2005), indicating strong rest-frame mid-IR emission. The source contains a weak C IV broad absorption line (BAL) system (Trump et al. 2006), a property possibly associated with enhanced far-IR emission (Priddey et al. 2007). Consideration of the broadband SED using a template-fitting approach led Hatziminaoglou et al. (2005, 2008) to conclude that it is hyperluminous ($L > 10^{13}\ L_{\odot}$) in the mid-IR, and suggested the source might have extreme luminosity at longer wavelengths.

2. OBSERVATIONS

SDSS 160705+533558 was initially observed with both the SCUBA bolometer array at the James Clerk Maxwell Telescope (JCMT), observing at 850 μm and 450 μm, and the MAMBO array at the IRAM 30 m, observing at 1200 μm. Observations at the JCMT were conducted on 2005 March 18 under Grade 1 conditions. The data were reduced using the SURF system with Mars as a primary calibrator and OH231.8

Table 1
Basic Data for SDSS 160705+533558

Data	Value
R.A.	16 07 05.16
Decl.	53 35 58.5
Redshift	3.653
u	23.61
g	19.35
r	18.15
i	18.14
z	17.98
J	0.36 ± 0.04
H	0.31 ± 0.06
K	0.34 ± 0.07
3.6 μm	0.40
4.5 μm	0.40
5.8 μm	0.66 ± 0.01
8.0 μm	1.33 ± 0.01
24 μm	6.31 ± 0.02
70 μm	22.2 ± 0.8
160 μm	<104 (5σ)
450 μm	220 ± 90 mJy
850 μm	31 ± 3
1200 μm	7.3 ± 0.9
$\log_{10}(L^{\rm IR}_{\rm total}/L_\odot)$	14.0–14.1
$\log_{10}(L^{\rm IR}_{\rm SB}/L_\odot)$	13.3–13.7
$\log_{10}(L^{\rm IR}_{\rm AGN}/L_\odot)$	13.8–13.9
SFR	3000–8000 $M_\odot$ yr^{-1}

Notes. Fluxes, basic data, and SED-fit results for SDSS 160705+533558. SDSS fluxes are given in AB magnitudes, all others are given as mJy. J, H, and K fluxes are from the Two Micron All Sky Survey. Errors on IRAC1 and 2 fluxes are of order 5%. See Hatziminaoglou et al. (2005) for more details on SDSS and *Spitzer* fluxes and I. Perez-Fournon et al. (2009, in preparation) for more details on submillimeter fluxes. Derived luminosities are given for the restframe 1–1000 μm waveband from our SED fitting.

as a secondary calibrator. The source was detected at 850 μm at 10σ confidence. An excess flux was obtained at 450 μm (2.5σ, 220 ± 90 mJy once calibration errors are included) though for the rest of this Letter, this is treated as a 3σ upper limit of 490 mJy. IRAM 30 m observations were carried out during the Winter 2004/2005 pool observing season using the 117 element version of the MAMBO array (Kreysa et al. 1998) operating at a wavelength of 1.2 mm (250 GHz) using standard on–off photometry observing mode in good conditions. Absolute flux calibration was established by observations of Mars and Uranus, resulting in a flux calibration uncertainty of about 20%. The data were reduced with standard procedures in the MOPSIC package developed by R. Zylka. More details of these observations are given in I. Perez-Fournon et al. (2009, in preparation). The fluxes are listed in Table 1.

Given the bright flux at 850 μm, we observed SDSS 160705+533558 with the Submillimeter Array (SMA; Ho et al. 2004). The source was observed using extended configuration on 2006 June 4, and in compact configurations on 2007 March 2 and 23 and 2007 June 4. Observations on 2007 March 23 and 2007 June 4 used all eight SMA antennas; the rest of the nights had only seven available. The resulting image created by combining all these data has UV coverage from 6.5 kλ to 218 kλ at the observed local oscillator (LO) frequency of 340 GHz. Observations were made in dry conditions, with τ_{225} ranging from 0.03 to 0.08. For all observations, the full 4 GHz bandwidth

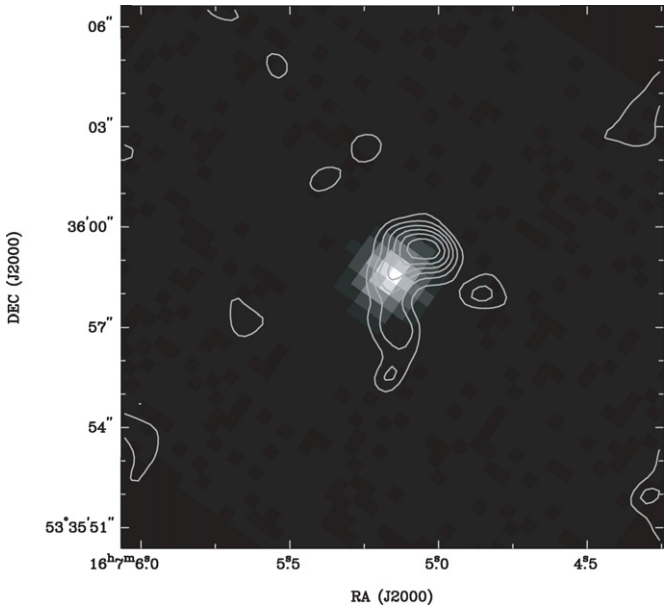


Figure 1. 850 μm image of SDSS 160705+533558. Grayscale optical image of SDSS 160705+533558, overlaid with contours from the SMA image. Contours are in steps of 1σ starting at 2σ, i.e., at fluxes of 2.4, 3.6, etc. mJy for the 1.2 mJy noise. Note the extended emission at submillimeter wavelengths and the offset of the submillimeter emission peak from the position of the optical quasar.

(2 GHz in each sideband separated by 10 GHz) was combined to achieve a total rms noise of 1.3 mJy in the final map. The SMA data were calibrated using the MIR software package developed at Caltech and modified for the SMA. Gain calibration was performed using the nearby quasars 1642+689, 1419+543, and 3C345. Absolute flux calibration was performed using real-time measurements of the system temperatures with observations of Titan and Neptune to set the scale, and bandpass calibration was done using 1921-293 or 3C273. Astrometric accuracy was determined by comparing the positions of the calibration objects 3C345 and 1642+689, using 3C345 as the reference and VLA astrometry to provide the true position. It was found to be accurate at the 0.″2 level. The data were imaged using Miriad (Sault et al. 1995), and further analysis was carried out using the KARMA software package.

3. RESULTS

3.1. Resolved Submillimeter Emission

Figure 1 shows the submillimeter emission in SDSS 160705+533558, derived from the SMA observations, overlaid on the SDSS optical image. The rest-frame far-IR emission is extended, consisting of a marginally resolved clump to the N and an arm extending to the S. There is also a possible companion source detected at the 3σ level 2.″2 (14.7 kpc) to the W. The peak of the far-IR emission is offset from the quasar position by ∼1.″5 to the N (∼10 kpc), with the emission arm extending roughly through the quasar position to the south. The overall length of the source, including the extended northern blob and the emission to the south, is 5.″4, or 36 kpc. The bright northern blob has a major axis size of ∼2.″4, corresponding to a size of 16 kpc. Comparison of the flux profile of this blob with that of the 1.″33 × 0.″85 beam shows that any unresolved component contributes at most 60% of its flux. The overall flux recovered from the interferometer at 850 μm is ∼12 mJy, which is significantly lower than the SCUBA flux, suggesting we have resolved emission on scales >4″.

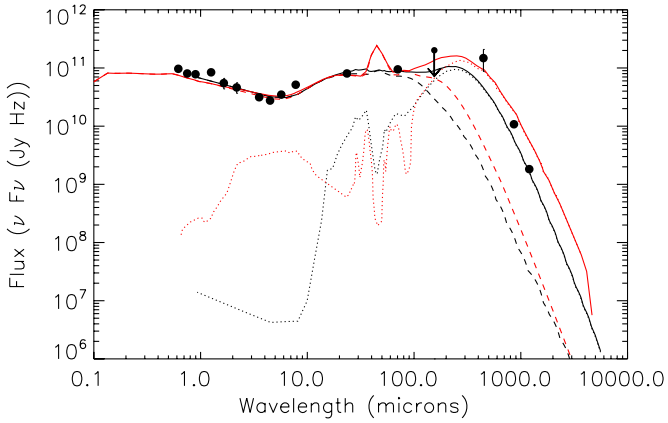


Figure 2. SED Fits for the IR-to-submillimeter fluxes of SDSS 160705+533558 We show the results for two different fits to the SED of SDSS 160705+533558, one using the methods of Farrah et al. (2003), the other those of Hatziminaoglou et al. (2008). The Farrah fits are shown in black; the Hatziminaoglou fits are shown in red. For both fits, we show the total SED as a solid line, the starburst component as a dotted line, and the AGN as a dashed line. The photometric data are shown as points, including the upper limit at 160 μm. There are significant differences between the fits and neither is a perfect match to the data, but these two independent methods reach the same conclusion that the mid-IR emission of this object is AGN dominated, while the far-IR/submillimeter emission, which we have resolved, is dominated by a starburst.

The spatial separation between the quasar and the peak of the submillimeter emission, and the extended nature of the latter component, strongly suggest a physical distinction between the processes powering the optical emission and the far-IR. Furthermore, the IRAC and MIPS 24 μm emission are centered at the position of the optical quasar, suggesting that emission in these bands is more strongly associated with the quasar than with the longer wavelength submillimeter emission. The 70 μm MIPS astrometry is not sufficiently accurate for a similar conclusion to be drawn. The optical/mid-IR is clearly associated with the AGN. This cannot be true for the extended submillimeter emission for which the most likely source is star formation of some kind.

3.2. Spectral Energy Distribution

Analysis of SEDs can provide constrains on the contributions of various components to the luminosity of galaxies. For the current source, where the imaging observations indicate distinct contributions from both an AGN and star formation, this is especially important. We obtain constraints on the total IR (1–1000 μm) luminosity and the contributions from the AGN and starburst by fitting the IR-to-submillimeter fluxes with model SEDs from a library of SEDs for starburst (Efstathiou et al. 2000) and AGN (Rowan-Robinson 1995) components. We use the methods described in Farrah et al. (2003) to determine the range of total starburst and AGN luminosities consistent with the data, and the star formation rate is derived from the starburst luminosity. The resulting best SED fit is shown in Figure 2, with the range of parameters giving adequate fits summarized in Table 1. We also apply the independent SED-fitting methods of Hatzminaoglou et al. (2008) to our source and these results are also shown in Figure 2. This approach fits the optical and mid-IR components of the SED using the grid of torus models from Fritz et al. (2006). Any excess that remains after this is fitted by an empirical starburst model selected from the following templates: Arp220, M82, NGC 1482, NGC 4102, NGC 5253, NGC 7714. Neither of the fits is perfect and there are significant detailed differences between the two results. However, both independent approaches reach the same broad conclusions about SDSS 160705+533558: (1) an AGN dominates its bolometric output as well as the rest-frame mid-IR (this matches earlier conclusions in Hatziminaoglou et al. (2008) based purely on *Spitzer* fluxes and our own conclusions based on the IRAC and MIPS 24 μm astrometry); (2) however, a massive obscured starburst is necessary to explain the strong rest-frame far-IR/submillimeter emission, with a star formation rate $> 1000\,M_{\odot}\,\mathrm{yr}^{-1}$. Our source thus appears to be a combination of AGN and starburst, with both components being very luminous in the infrared. The derived total infrared luminosity, $\sim 10^{14}\,L_{\odot}$, confirms that SDSS 160705+533558 is an HLIRG (Rowan-Robinson 2000) and that it is among the most luminous far-IR objects known.

4. DISCUSSION

The discovery of extended rest-frame far-IR emission, on scales from 16 to 36 kpc, offset from the optical quasar is unexpected. The majority of observations of distant submillimeter galaxies (SMGs) to date have revealed small-scale or unresolved emission at these wavelengths (e.g., Younger et al. 2008a, 2008b; Tacconi et al. 2006) consistent with the "Maximum Starburst" model for galactic bulge formation described by Elmegreen (1999). If we scale the source sizes measured in Tacconi et al. (2006) to that expected for the maximum SFR derived for SDSS 160705+533558, we would expect a source 3.4 kpc in size rather than the 16 kpc found for the brightest emission region or the 36 kpc found for the overall structure. Our source is thus inconsistent with this "Maximum Starburst" model, suggesting that this is not a complete model for the high-redshift submillimeter population.

Some submillimeter-luminous high-redshift AGNs are extended in the submillimeter. BRI 1202-0725, one of the few high-redshift submillimeter-AGNs with a higher luminosity than SDSS 160705+533558, consists of a pair of sources separated by 4″, the brightest of which has a size of $\sim 3'' \times 0\farcs7$ (Omont et al. 1996). Other resolved far-IR luminous quasars include PSS J2322+1944 (Carilli et al. 2002a) at $z = 4.12$, whose CO emission is found to be extended on a scale of 2″, BRI 1335-0417 at $z = 4.4$, which is resolved into two components separated by $\sim 1''$ (Carilli et al. 2002b), and 4C41.17 which contains two CO components $1\farcs8$ apart (De Breuck et al. 2005). The lensed quasar APM 08279+5255, in contrast, is unresolved by a $0\farcs7 \times 0\farcs65$ beam (Krips et al. 2007). However, unlike the current source all these objects have their AGNs closely associated with one of the far-IR or CO peaks. We do not yet have CO data for our source, but we do not expect the CO distribution to be radically different from the 850 μm continuum emission, so once again SDSS 160705+533558 is unusual.

One possible equivalent object is 4C60.07, a $z = 3.8$ submillimeter bright (23.8 ± 3.5 mJy) radio galaxy studied by Ivison et al. (2008), whose far-IR luminosity is less than that of SDSS 160705+533558, where the submillimeter components lie 10–30 kpc on the plane of the sky away from the radio core. This source is thought to be a young merger between two high mass objects. The host of the offset radio nucleus is thought to have exhausted or expelled its molecular gas, while the other is gas rich and responsible for much of the submillimeter emission. The remaining submillimeter emission comes from gas rich tidally stripped material falling toward the radio core.

4C60.07 and SDSS 160705+533558 are far from identical and more information regarding the molecular gas and underlying old stellar population in our source are needed before we can draw a direct comparison, but we speculate that the extended submillimeter tail in our source is a tidal structure similar to that suggested for 4C60.07. The object might thus be in the early stages of a merger between a galaxy rich in molecular material and a dust-poor galaxy which hosts a supermassive black hole. The interaction has triggered star formation in the dust rich system and quasar activity through fueling the supermassive black hole. The differences between this system and more conventional SMGs would then be a result of the early stage of the merger. An alternative is the possibility that some or all of the star formation in this system is triggered by interaction between jets from the AGN and molecular material (e.g., Klamer et al. 2004). Observations at radio wavelengths in search of these jets would be needed to test this idea.

5. CONCLUSIONS

The $z = 3.65$ quasar SDSS 160705+533558 has been found to be bright in both the far-IR and submillimeter. SED fitting indicates that the rest-frame far-IR luminosity is largely due to star formation with an inferred star formation rate of a few $10^3\ M_\odot\ \mathrm{yr}^{-1}$. SMA imaging has found the submillimeter emission to be extended in a linear north–south structure $\sim$36.2 kpc long, dominated by a clump of size 16 kpc to the north. The AGN is located roughly in the middle of the linear structure, but away from the submillimeter peak. We conclude that an early stage merger between two galaxies, one of which is gas rich, while the other hosts a supermassive black hole, is the most likely explanation for the unusual extended emission given the data currently available. Further observations of this unusual source, from optical to radio, are underway.

This work was funded in part by PPARC/STFC and NASA. The Submillimeter Array is a joint project between the Smithsonian Astrophysical Observatory and the Academia Sinica Institute of Astronomy and Astrophysics and is funded by the Smithsonian Institution and the Academia Sinica. The James Clerk Maxwell Telescope is operated by The Joint Astronomy Centre on behalf of the Science and Technology Facilities Council of the United Kingdom, the Netherlands Organisation for Scientific Research, and the National Research Council of Canada. Data were taken as part of JCMT project M05AU24. The authors thank Joe Silk, George Bendo, and Pierre Chanial for useful discussions and the anonymous referee whose comments have significantly improved the paper.

REFERENCES

Alexander, D. M., Bauer, F. E., Chapman, S. C., Smail, I., Blain, A. W., Brandt, W. N., & Ivison, R. J. 2005, ApJ, 632, 736
Armus, L., et al. 2007, ApJ, 656, 148
Carilli, C. L., et al. 2002a, ApJ, 575, 145
Carilli, C. L., et al. 2002b, AJ, 123, 1838
Clements, D. L., et al. 2008, MNRAS, 387, 247
Coppin, K., et al. 2006, MNRAS, 372, 1621
de Breuck, C., Downes, D., Neri, R., van Breugel, W., Reulent, M., Omont, A., & Ivison, R. 2005, A&A, 430, L1
Desai, V., et al. 2007, ApJ, 669, 810
Dye, S., et al. 2008, MNRAS, 386, 1107
Eales, S. A., et al. 2000, AJ, 120, 2244
Efstathiou, A., Rowan-Robinson, M., & Siebenmorgan, R. 2000, MNRAS, 313, 734
Elmegreen, B. G. 1999, ApJ, 517, 103
Farrah, D., Afonso, J., Efstathiou, A., Rowan-Robinson, M., Fox, M., & Clements, D. 2003, MNRAS, 343, 585
Farrah, D., et al. 2007, ApJ, 667, 149
Fixsen, D. J., et al. 1998, ApJ, 508, 123
Fritz, J., Franceschini, A., & Hatziminaoglou, E. 2006, MNRAS, 366, 767
Haring, N., & Rix, H.-W. 2004, ApJ, 604, L89
Hatziminaoglou, E., et al. 2005, AJ, 129, 1298
Hatziminaoglou, E., et al. 2008, MNRAS, 386, 1252
Ho, P. T. P., Moran, J. M., & Lo, K. Y. 2004, ApJ, 616, 1
Hughes, D. H., et al. 1998, Nature, 394, 241
Ivison, R. J., et al. 2008, MNRAS, 390, 1117
Klamer, I. J., Ekers, R. D., Sadler, E. M., & Hunstead, R. W. 2004, ApJ, 612, L97
Kreysa, E., et al. 1998, in Proc. SPIE 3357, 319
Krips, M., Peck, A. B., Sakamoto, K., Petitpas, G. B., Wilner, D. J., Matsushita, S., & Iono, D. 2007, ApJ, 671, L5
Lonsdale, C., et al. 2004, ApJS, 154, L54
Omont, A., Petitjean, P., Guiloteau, S., McMahon, R. G., Solomon, P. M., & Pecontal, E. 1996, Nature, 382, 428
Priddey, R., Isaak, K. G., McMahon, R. G., & Omont, A. 2003, MNRAS, 339, 1183
Priddey, R., Gallagher, S. C., Isaak, K. G., Sharp, R. G., McMahon, R. G., & Butner, H. M. 2007, MNRAS, 374, 867
Puget, J.-L., et al. 1996, A&A, 308, L5
Rowan-Robinson, M. 1995, MNRAS, 272, 737
Rowan-Robinson, M. 2000, MNRAS, 316, 885
Sault, R. J., Teuben, P. J., & Wright, M. C. H. 1995, ASPC, 77, 433
Smail, I., Ivison, R. J., & Blain, A. W. 1997, ApJ, 490, L5
Stevens, J. A., Page, M. J., Ivison, R. J., Smail, I., & Carerra, F. J. 2004, ApJ, 604, L17
Tacconi, L. J., et al. 2006, ApJ, 640, 228
Trump, J. R., et al. 2006, ApJS, 165, 1
Younger, J. D., et al. 2008a, MNRAS, 387, 707
Younger, J. D., et al. 2008b, ApJ, 688, 59